Research article

High expression of PDCD11 in colorectal cancer and its correlation with the prognosis and immune cell infiltration

Xiongfeng Li [a,1], Gaowa Sharen [b,1], Minjie Zhang [c,1], Lei Zhang [a], Kejian Liu [a], Yu Wang [a], Haidong Cheng [a,*], Mingxing Hou [a,**]

[a] *Department of Gastrointestinal Surgery, Affiliated Hospital of Inner Mongolia Medical University, Hohhot, 010059, Inner Mongolia, China*
[b] *Department of Pathology, Affiliated Hospital of Inner Mongolia Medical University & Department of Pathological Anatomy, College of Basic Medicine of Inner Mongolia Medical University, Hohhot, 010059, Inner Mongolia, China*
[c] *Department of Ultrasound, Affiliated Hospital of Inner Mongolia Medical University, Hohhot, 010059, Inner Mongolia, China*

A R T I C L E   I N F O

A B S T R A C T

Objective: To undertake a comprehensive assay of PDCD11 expression in colorectal cancer (CRC) and its association with prognosis and immune cell infiltration (ICIN) utilizing bioinformatics tools.
Methods: The PDCD11 expression in CRC and pan-cancer was quantified through datasets from TCGA and GEO databases, and the assay was conducted through R software and the GEPIA database. Moreover, mRNA and protein expression data of PDCD11 were attained from the HPA database. It was attempted to establish protein-protein interaction networks of PDCD11 via the STRING and GeneMANIA databases. The association of PDCD11 expression with CRC staging was evaluated through R software, while its association with CRC and pan-cancer prognosis was figured out via the GEPIA database. Furthermore, the relationship of PDCD11 expression with ICIN was assayed using R software and the TIMER database. Additionally, the influences of PDCD11 knockdown on the proliferation, apoptosis, and migration of colon cancer RKO cell lines was evaluated.
Results: PDCD11 exhibited elevated expression in CRC and various other malignancies, potentially indicating a promotive role in cancer progression. Overexpression of PDCD11 was found to correlate with attenuated overall survival in CRC and other malignancies. Moreover, PDCD11 demonstrated promising predictive capabilities for distinguishing between tumor and non-tumor tissues. The positive association of high PDCD11 expression with the infiltration of neutrophils, dendritic cells, CD8+ T cells, CD4+ T cells, and macrophages, as well as with the expression of immune checkpoint molecules CTLA4 and PD-1 was noteworthy. Lentivirus-mediated PDCD11 knockdown suppressed RKO cell proliferation, colony formation, and migration, while triggered apoptosis in these cells.
Conclusion: The outcomes unveiled the noticeable function of PDCD11 in CRC and various other malignancies, emphasizing its potential as a prognostic biomarker and therapeutic target.

* Corresponding author.Department of Gastrointestinal Surgery, Affiliated Hospital of Inner Mongolia Medical University, No. 1 Tongdao North Road, Hohhot, 010059, Inner Mongolia, China.
** Corresponding author. Department of Gastrointestinal Surgery, Affiliated Hospital of Inner Mongolia Medical University, No. 1 Tongdao North Road, Hohhot, 010059, Inner Mongolia, China.
E-mail addresses: chd2476@163.com (H. Cheng), hmx6412@163.com (M. Hou).
[1] Xiongfeng Li, Gaowa Sharen and Minjie Zhang contributed equally to this study.

1. Introduction

Colorectal cancer (CRC) represents a prevalent malignancy within the lower gastrointestinal tract, positioning as the third most frequent cancer and the second fundamental cause of cancer-related mortality in the global scale [1]. The incidence of CRC in China is increasing yearly, which is a malignant tumor ranking first in morbidity and fourth in mortality rate among digestive system diseases in China [2]. It threatens people's lives and exerts a heavy burden particularly on society. At present, the primary therapies for CRC involve surgery, radiotherapy, and chemotherapy, while targeted molecular therapy plays a secondary function [3]. These treatments are generally effective only for early-stage CRC cases. Due to the lack of symptoms in early-stage CRC cases and the imperfect early screening system, CRC cases cannot be diagnosed in the early stages and have progressed to the middle and late stages when symptoms appear [4]. Despite substantial advancements in multidisciplinary treatment approaches for CRC in recent years, advanced-stage CRC cases' overall prognosis has not accompanied by remarkable improvement, with the 5-year survival rate lingering around a mere 14 % [5]. This outcome underscores the critical need for the identification and characterization of genes implicated in CRC's pathogenesis and progression. Such studies are paramount for the discovery of potential molecular markers and therapeutic targets, which are essential for the prevention and precise treatment of CRC, as well as for the accurate assessment of patient prognosis.

PDCD11 is a member of the programmed cell death (PDCD) family, also known as apoptosis-linked gene 4 (ALG4), which is a class of proteins associated with tumor development and highly conserved in evolution [6]. The PDCD11 protein is distinguished by a series of S1 RNA-binding domains at its N-terminus, spanning approximately 1400 amino acids, and is complemented by a tetratricopeptide repeat (TPR) domain situated at the C-terminus [7]. The S1 RNA-binding domains at the N-terminus facilitate PDCD11's interaction with pre-rRNA, orchestrating a pivotal role in the intricate processes of rRNA processing and assembly within the nucleolus [8–10]. Additionally, it interacts with Exonuclease-1 and enhances Fas expression, thereby promoting cell apoptosis [11,12]. Recent discoveries have elucidated that PDCD11 engages with NF-κB subunits to inhibit inflammatory cytokines' expression levels while concurrently activating the TGFβ1 pathway. This interaction plays a notable function in modulating microglia differentiation during zebrafish development [13]. The PDCD family is widely distributed in human tissues and cells and regulates apoptosis. It is demonstrated that the PDCD family can regulate tumor cell viability through different signaling pathways, and the deletion or overexpression of some family members may cause lesions, indicating that the PDCD family plays a noticeable function in diverse tumors' occurrence and progression [14]. Unveiling the function of PDCD11 in CRC could have profound implications for patient care. Firstly, it might serve as a robust molecular marker for early detection, enabling clinicians to identify high-risk individuals and initiate timely interventions. Additionally, understanding PDCD11's involvement in CRC progression may pave the way for targeted therapies. Given the recent successes of targeted molecular therapies for diverse malignancies, elucidating mechanisms of PDCD11 could enhance the therapeutic modalities particularly for CRC patients, potentially improving their outcomes and quality of life [15]. Moreover, the interaction of PDCD11 expression with immune cell infiltration (ICIN) in CRC is an area ripe for exploration. Immune checkpoint molecules, e.g. programmed death-1 (PD-1), have revolutionized cancer therapy [16]. Investigating how PDCD11 could influence immune responses in the tumor microenvironment could unveil novel immunotherapeutic targets.

In the field of genetics, CRC is one of the most studied tumors [17]. From benign development to malignant transformation of diseased tissues, genetic information undergoes a series of changes, such as chromosomal abnormalities, gene mutations, and epigenetic alterations, which may result in inactivating tumor suppressor genes, mutation of DNA repair genes, and activation of oncogenes. In addition, various personal habits and lifestyle choices, involving adherence to a high-fat diet, excessive consumption of red meat, smoking, and alcohol intake, have been recognized as contributory factors in the etiology of CRC [18,19]. CRC is an immunogenic disease, and its occurrence and development are related to host immune deficiencies, such as chromosomal abnormalities, genetic mutations, and epigenetic changes [20]. During disease progression, immune cells change their phenotype and function over time, thereby making the immune microenvironment as both "tumor suppressor" and "tumor promotor". Since cytotoxic T lymphocyte infiltration is associated with cancer cases' survival, an immune scoring system was established [21]. It is noteworthy that the tumor immune score is a prognostic indicator particularly for CRC patients, independent of patients' TNM stage, indicating that patients with a high tumor immune score have prolonged overall survival (OS) [22]. Extensive research has elucidated the multifaceted functions of the immune system in thwarting tumorigenesis and tumor progression. It enhances antiviral defenses, mitigates pro-inflammatory conditions, eradicates malignant cells, and engages in continuous immune surveillance [21]. Recent outcomes have resulted in substantial advancements in the assessment of diverse immune cell subsets, contributing to a refined understanding of their prognostic implications in oncology. Bruni D et al. pointed out that CD8^{+} T cells, CD3^{+} T cells and T helper cells (TH1, TH2, TH17, Treg, TFH) can be used as immune background parameters for tumor prognosis as predicting biomarkers [22]. The revelation that suppressing immune checkpoints enables tumors to evade immune surveillance has resulted in a groundbreaking revolution in anti-tumor therapy, and the specific binding between anti-programmed death 1 (PD-1) and anti-programmed cell death ligand 1 (PD-L1) can inhibit the production of IL-2 by T cells and increase T lymphocyte-dependent apoptosis [23]. Immune checkpoint inhibitors (ICIs), particularly those targeting the PD-1/PD-L1 axis, have markedly elevated cancer patients' prognostic outcomes, because disrupting immune resistance and activating cytotoxic T cells can lead to durable clinical benefits for patients with refractory solid tumors, including a small proportion of patients with metastatic CRC [20,22]. Immune cells exhibiting anti-tumor properties, encompassing CD4^{+} T cells, Th17 cells, CD8^{+} T cells, and CD4^{+} regulatory T cells (Tregs), have emerged as focal points for immunotherapeutic interventions and prognostic assessments in cancer management [21]. Although there are few previous studies about the expression and regulation of PDCD11 in tumor tissues, our hypothesis suggests a potential contribution of PDCD11 to the promotion of CRC and its impact on tumor prognosis, given its classification as a member of the programmed death family.

It is a widely held belief that the immune system, when triggered by tumor cells, engages in immune surveillance and defense

mechanisms, thereby suppressing malignancy progression [15]. However, the dichotomous nature of immune system activation presents both advantageous and deleterious outcomes. Mounting evidence unveiled that numerous immune cells recruited by advanced tumors can instigate inflammation and the secretion of cytokines and chemokines, resulting in promoting tumor growth, metastasis, invasion, and pathological angiogenesis [16]. The exploration of immune-related mechanisms holds significant promise for the advancement of cancer therapies [17]. For instance, the immune checkpoint molecule PD-1 has been recognized as a critical target for cancer therapy [18], with several PD-1 inhibitors receiving approval from the FDA for the therapy of malignant melanoma [19]. Furthermore, tumors' infiltration by immune cells has emerged as a critical determinant impacting the prognostic trajectory of the disease [20]. Despite these advancements, the expression and regulatory mechanisms of PDCD11 in malignant tumors remain inadequately explored. Bridging this knowledge gap is essential for elucidating the specific role of PDCD11 in CRC. By analyzing the differential expression levels of PDCD11 in CRC tissues compared to normal tissues, PDCD11 could potentially be identified as a novel molecular marker for early detection. Early detection is paramount for improving patient outcomes by enabling prompt intervention and treatment. Consequently, this investigation aimed to quantify the expression levels of PDCD11 in CRC tissues relative to normal tissues and to figure out the correlation of PDCD11 expression with ICIN in CRC. Such research may yield novel insights, aiding clinicians in enhancing treatment strategies and prognostic outcomes for CRC cases.

2. Materials and methods

2.1. Collection and analysis of data

The colon cancer and pan-cancer datasets utilized in this study were derived from the RNAseq data (level 3 HTSeq-FPKM format) associated with the respective projects within TCGA (The Cancer Genome Atlas). To ensure robust analytical integrity, the RNAseq data in FPKM (Fragments Per Kilobase per Million) format were subjected to a log2 transformation. Additionally, the GSE39582 gene set was acquired from the NCBI-GEO database, providing a comprehensive foundation for gene expression analysis. Expression data pertaining to PDCD11 and its mRNA levels in normal tissues were precisely attained from the Human Protein Atlas (HPA) database, offering valuable insights into baseline expression profiles.

2.2. Analysis of expression difference

The RNAseq data in level 3 HTSeq-FPKM format from the colon cancer and pan-cancer projects within the TCGA database were subjected to a log2 transformation. Subsequent statistical examinations and illustration were performed through R 3.6.3 alongside the ggplot2 3.3.3 package. Differential analysis for paired samples in colon cancer employed the paired sample *t*-test, while it was attempted to analyze unpaired samples through the Mann-Whitney *U* test. In the context of pan-cancer analyses, the Wilcoxon signed-rank test was employed to assay paired samples, whereas unpaired samples were statistically assayed through the Mann-Whitney *U* test. The significance thresholds were delineated with a remarkable stratification as follows: "ns" was indicative of P-values upper or equal to 0.05; a single asterisk (*) was employed to denote P-values subordinated 0.05; double asterisks (**) were utilized for P-values subordinated 0.01; triple asterisks (***) were reserved for P-values subordinated 0.001. Data originating from TCGA and GTEx databases, after undergoing standard preprocessing [24], were subjected to differential analysis via the "Expression DIY" module in the GEPIA database. This rigorous analytical pipeline ensured robust and reliable insights into the differential expression patterns across the datasets.

2.3. Expression of PDCD11 mRNA and protein in normal tissues and immunohistochemical analysis

The expression data of PDCD11 in normal tissues and the immunohistochemical results in colon cancer and para-carcinoma tissues were obtained from the "Tissue" module and "Pathology" module of the HPA database.

The HPA database was launched in 2003 with funding from the Knut and Alice Wallenberg Foundation. The "Tissue" module stores immunohistochemical data for protein expression in 44 types of normal human tissue and RNA-seq data for 256 types of normal tissues. The "Pathology" module stores mRNA and protein expression data for 17 human cancers.

2.4. PPI construction

The STRING and GeneMANIA databases were utilized to establish the protein-protein interaction (PPI) networks of PDCD11. In the Species option, check the *Homo sapiens* option, and the parameter settings are all default parameters.

2.5. Screening for PDCD11-related molecules and correlation analysis

Three distinct methodologies were employed for the screening of related molecules: 1. Initial screening involved inputting PDCD11 into the STRING database to recognize the top 30 molecules exhibiting protein interactions. These molecules were subsequently subjected to correlation analysis. 2. CRC cases in TCGA database were categorized into groups of high and low PDCD11 expression on the basis of median value. Differential expression analysis of coding genes was thereafter conducted between these groups using the DESeq2 R package. Genes with LogFC>1 or LogFC < −2 and adj.P.val<0.05 were utilized for further correlation analysis. 3. It was attempted to undertake Pearson correlation analysis on PDCD11 and other molecules in CRC through the R package stats (version

3.6.3). The selection of top 50 coding genes was carried out for subsequent investigation.

Statistical examinations and illustration were executed using R 3.6.3 software, with visualization predominantly accomplished using the ggplot2 3.3.3 package. Spearman correlation analysis of CRC data from the TCGA database was represented graphically as a heatmap. This heatmap was bifurcated, illustrating the z-score transformations of both PDCD11 and the other genes. The significance thresholds were delineated with a remarkable stratification as follows: "ns" was indicative of P-values upper or equal to 0.05; a single asterisk (*) was employed to denote P-values subordinated 0.05; double asterisks (**) were utilized for P-values subordinated 0.01; triple asterisks (***) were reserved for P-values subordinated 0.001.

2.6. GO and KEGG enrichment analysis

R 3.6.3 software served as the primary tool for conducting statistical examinations and illustration. Visualization tasks were predominantly implemented using the ggplot2 3.3.3 package, while the clusterProfiler 3.14.3 package was employed for comprehensive analysis of the selected datasets. It was attempted to undertake GO and KEGG enrichment analyses on the molecules recognized by the three aforementioned screening strategies [25]. The illustration of outcomes was executed through bubble charts, where the bubble size corresponded to the Count value, the color intensity of the bubbles reflected the magnitude of the p.adjust value, and the X-axis was representative of the GeneRatio. This visualization approach provided a notable depiction of the enrichment analysis outcomes, enabling a clear interpretation of the data.

2.7. Correlation analysis on prognosis

Leveraging R 3.6.3 software for comprehensive statistical examinations and illustration, and primarily utilizing the ggplot2 3.3.3 package for detailed graphical representation, an in-depth correlation analysis of PDCD11 expression with CRC progression was conducted across the M and N stages. This analysis was grounded in RNAseq data and corresponding clinical data in level 3 HTSeq-FPKM format from TCGA-CRC Project. To maintain analytical rigor, datasets lacking clinical information were systematically excluded. The statistical analysis employed Dunn's test for multiple hypothesis testing, with significance levels precisely adjusted using the Bonferroni correction method.

It was attempted to undertake ROC curve analysis with precision using the pROC 1.17.0.1 R package for computational evaluation and the ggplot2 3.3.3 R package for visualization. In this analytical framework, the X-axis was indicative of the false positive rate (FPR), while the Y-axis depicted the true positive rate (TPR).

Survival analysis was precisely implemented through the "Survival" module in the GEPIA database. The "Overall Survival" option was selected in the Methods, and "Median" was employed for the Group Cutoff option [24]. This approach facilitated a robust, median-based stratification of patient cohorts, enabling a detailed comparison of survival outcomes.

2.8. Correlation analysis on ICIN

The enrichment of ICIN in CRC was precisely computed through the TIMER database [26,27]. This platform enabled the quantification of six distinct types of immune-infiltrating cells, namely B cells, CD4$^+$ T cells, CD8$^+$ T cells, neutrophils, macrophages (MACs), and dendritic cells (DCs), by inputting gene expression profiling data from tumor samples. To approve the robustness of the outcomes, EPIC, an advanced analytical method for deducing the proportions of immune cells and cancer cells from comprehensive tumor gene expression data, was employed for validation [28].

A broader scope of ICIN was assessed by incorporating a total of 24 immune cell types [29]. The relative enrichment scores of these immune cells in CRC were calculated through ssGSEA alongside the GSVA R package [30], demonstrating a notable view of the immune landscape in the tumor microenvironment. Spearman correlation analysis was thereafter performed to figure out the relationship of PDCD11 expression with the infiltration levels of these immune cells, providing deeper insights into the immunological context of PDCD11 expression in CRC.

2.9. Correlation analysis on immune checkpoints

Immune checkpoint correlation analysis was performed through the "Correlation Analysis" module available on the GEPIA database utilizing Pearson correlation analysis.

2.10. Cell cultivation

The source of human CRC cell lines, herein (HCT116, LoVo, RKO, and SW480, were the Cell Bank of the Shanghai Institutes for Biological Sciences, affiliated with the Chinese Academy of Sciences. Their cultivation was implemented in RPMI-1640, which was enriched with 10 % fetal bovine serum (FBS) and 1 % antibiotics (penicillin/streptomycin) to maintain sterility and support cell growth. Their incubation in a precisely controlled environment was performed particularly at 37 °C with 5 % carbon dioxide, ensuring optimal conditions for cellular metabolism and proliferation. This precise setup facilitated the reliable harvesting and maintenance of the CRC cell lines for subsequent experimental assays.

2.11. Lentiviral preparation

Third-passage RKO cells, cultivated to 80 % confluence, underwent transduction with two lentiviral vectors encoding PDCD11-specific shRNA and scrambled shRNA controls. The transduction process was conducted overnight at a multiplicity of infection (MOI) of 20, facilitated by the addition of 5 μg/mL polybrene to enhance viral entry. Following the initial 24-h transduction period, the cells were maintained in DMEM attained from Sigma-Aldrich that was headquartered in St. Louis (MO, USA), which was enriched with 10 % FBS. 72-h post-infection, GFP expression in RKO cells was visualized through an A1 confocal laser scanning microscope attained from Nikon that was headquartered in Japan, with green fluorescence indicating successful transduction of GFP-positive cells. To isolate transduced cells, a selection process involving puromycin (1 μg/mL) was employed, allowing for the recognition and expansion of puromycin-resistant colonies. These colonies were thereafter precisely expanded and subjected to rigorous analysis. The efficacy of PDCD11 knockdown was assayed utilizing quantitative real-time polymerase chain reaction (qRT-PCR) to quantify mRNA level, coupled with immunoblotting to evaluate protein expression. This multifaceted approach ensured a thorough validation of PDCD11 gene silencing.

2.12. Lentiviral transduction

At the third passage, the culture of RKO cells, particularly at 80 % confluence, was performed via sophisticated transduction process involving two lentiviral vectors: one containing PDCD11-specific shRNA and the other containing scrambled shRNA controls. This transduction occurred overnight with a carefully calculated MOI of 20, enriched with 5 μg/mL polybrene to enhance viral entry efficiency. Following a precisely timed 24-h incubation, it was attempted to culture RKO cells in a DMEM attained from Sigma-Aldrich that was enriched with 10 % FBS. After a precisely monitored 72-h infection, the expression of GFP in the RKO cells was precisely quantified under an A1 confocal laser scanning microscope (Nikon). The detection of green fluorescence signaled successful transduction, indicating the presence of GFP-positive cells. Subsequently, transduced RKO cells underwent a stringent selection process employing puromycin at a concentration of 1 μg/mL, isolating cells resistant to puromycin.

Colonies exhibiting resistance were painstakingly hand-picked, expanded, and subjected to comprehensive assays. The potency of PDCD11 knockdown was precisely figured out through a combination of sophisticated techniques, including qRT-PCR and immunoblotting analysis. These assays provided a multifaceted evaluation of PDCD11 gene silencing efficacy.

2.13. RNA preparation and qRT-PCR

CRC cells were subjected to total RNA extraction through a commercial Trizol reagent attained from TaKaRa that was headquartered in Dalian (China) on the basis of instructions outlined by the manufacturer. Subsequently, it was attempted to synthesize cDNA through the cDNA Reverse Transcription kits attained from Thermo Fisher Scientific that was headquartered in the USA. The cDNA amplification was thereafter performed via qRT-PCR using the SYBR Green Mix attained from Thermo Fisher Scientific on the ABI7500 Sequence Detection System attained from Applied Biosystems (USA). The specific primer sets for PDCD11 were utilized: forward primer sequence, 5′-GCCACACCAAGCCACGATAA-3′, and reverse primer sequence, 5′-ACTGCCTGCACATCCTTCTC-3'. It was attempted to normalize PDCD11 expression to GAPDH expression, for which the forward primer sequence was 5′-CTCAACTACATGGTCTACATGTTCCA-3′, and the reverse primer sequence was 5′-CTTCCCATTCTCAGCCTTGACT-3'. The findings were assayed utilizing the $2^{-\Delta\Delta Ct}$ method, where $\Delta Ct = Ct_{PDCD11} - Ct_{GAPDH}$.

2.14. Immunoblotting analysis

RKO cells underwent lysis in an enhanced RIPA buffer enriched with the protease inhibitor phenylmethylsulfonyl fluoride (PMSF) attained from BOSTER that was headquartered in Wuhan (China). Subsequent to lysis, the cellular extracts underwent separation through electrophoresis on a 10 % SDS-PAGE gel, after which they were transferred onto a membrane. Immunoblotting was performed through primary antibodies targeting the proteins of interest, followed by being incubated with either HRP-conjugated goat anti-mouse or anti-rabbit IgG secondary antibodies (AS1107 and AS1106) attained from ASPEN Biotechnology that was headquartered in Wuhan (China). The visualization of the immunoblots was performed using high-sensitivity enhanced chemiluminescence (ECL) reagents attained from BOSTER, employing an Amersham Imager 600 (USA). Following visualization, the densitometric analysis of the immunoblots was implemented utilizing ImageJ software (USA), enabling precise quantification of the protein bands and providing insights into the expression levels of the proteins of interest.

2.15. Celigo image cytometry

RKO cells were liberated from culture dishes via trypsinization utilizing 0.25 % trypsin attained from Thermo Fisher Scientific, which were precisely resuspended in DMEM, and distributed into individual wells of a 96-well plate at a seeding density of 2000 cells per well. These plates were thereafter transferred to a precisely controlled carbon dioxide incubator maintained at 37 °C, where they remained for a continuous incubation period spanning 5 consecutive days. Utilizing the advanced Celigo Image Cytometer attained from Nexcelom Bioscience that was headquartered in Lawrence (MA, USA), the number of cells was precisely monitored each day through a series of scans capturing green fluorescence.

2.16. Colony formation assay

For the rigorous evaluation of colony formation potential, RKO cells were precisely dissociated into single-cell suspensions utilizing 0.25 % trypsin and subsequently plated at a density of 800 cells in a 60-mm dish. In the presence of optimized conditions within a 5 % carbon dioxide incubator set at 37 °C, these cells were allowed to proliferate undisturbed until the formation of distinct and visible colonies. Subsequently, it was attempted to twice rinse colonies with phosphate-buffered solution (PBS) to exclude any non-adherent cells, followed by being fixed for 15 min with 4 % paraformaldehyde. A 10-min staining with 0.5 % crystal violet was performed, after which colonies were quantified under a BZ-X710 microscope attained from Keyence Corp. That was headquartered in Osaka (Japan), ensuring accurate assessment of colony formation potential with a prerequisite of at least 50 cells per colony.

2.17. MTT assay

In the MTT assay, it was attempted to plate RKO cells in a 96-well plate at a seeding density of 2500 cells per well. At defined time intervals spanning days 1 through 5, it was attempted to add MTT solution (10 µL, 5 mg/ml) attained from Sigma-Aldrich to each well, followed by a precise 4-h incubation particularly at 37 °C. Upon completion of the incubation, formazan crystals were accurately solubilized, and addition of 150 µL of DMSO to each well was implemented. Cell viability, serving as an indicator of metabolic activity, was quantified through measuring the optical density (OD) at 490 nm via a microplate reader.

2.18. Flow cytometric analysis for apoptosis

To thoroughly evaluate cell apoptosis, an annexin V-allophycocyanin (APC) apoptosis detection kit, attained from Ebioscience that was headquartered in San Diego (CA, USA), was employed on the basis of the instructions outlined by the manufacturer. The suspension of RKO cells in $1 \times$ binding buffer (Thermo Fisher Scientific) was implemented, and a precise 100 µL of cell suspension (1×10^6 cells/mL) was incorporated with 10 µL of annexin V-APC. Following 15-min incubation in darkness particularly at room temperature, it was attempted to add 400 µL of binding buffer, and the samples were assayed through a flow cytometer attained form BD Biosciences that was headquartered in San Jose (CA, USA). The collected data were proceeded through FlowJo software (BD Biosciences).

2.19. Wounding healing assay

The cultivation of RKO cells in a serum-free DMEM was executed, and their seeding into 6-well plates was performed particularly at a density of 5×10^5 cells per well. Subsequently, a precise scratch measuring 10 µL in width was created along the central axis of each well through a sterile pipette tip. This ensured uniformity in the scratch dimensions across all wells. The dynamic process of wound closure was monitored utilizing the Celigo Image Cytometer attained from Nexcelom Bioscience, which scanned for green fluorescence in the wound area at various time points spanning from 0 to 48 h post-incubation with serum-free DMEM.

2.20. Transwell migration assay

For the cell migration assay, Transwell chamber systems incorporated into a 24-well plate, featuring pores of 8-µm diameter, were employed. The adjustment of RKO cells was conducted in serum-free DMEM (100 µL), and a precisely measured 200 µL of the cell suspension was gently introduced into the upper chambers. Following a precise 24-h incubation particularly at 37 °C, the cells that had migrated to the lower chamber, containing DMEM supplemented with 10 % FBS attained from Invitrogen, were fixed with 4 % paraformaldehyde and subsequently stained with 0.05 % crystal violet. The quantification of stained cells was performed across six randomly selected fields per well via an inverted BZ-X710 microscope attained from Keyence Corp.

2.21. Statistical analysis

Statistical analysis was executed utilizing SPSS 21.0 software that was developed by IBM and headquartered in Armonk (USA), incorporating a comprehensive array of statistical tests, involving one-way analysis of variance (ANOVA) adjusted with Tukey's test, paired or unpaired t-tests, and repeated measurements ANOVA with Bonferroni corrections as appropriate. It was attempted to express the data in the format of mean $\pm$ standard deviation, and P subordinated 0.05 was regarded to signify statistical significance.

3. Results

3.1. Differential expression of PDCD11 in CRC and pan-cancer

To figure out the function of PDCD11 in carcinogenesis, the expression of PDCD11 in CRC and pan-cancer was examined. We analyzed RNA-seq data of CRC in TCGA database and a colon cancer dataset GSE39582 in the GEO database, and the outcomes unveiled that PDCD11 expression was elevated in cancerous tissues relative to para-carcinoma tissues in both paired and unpaired CRC samples (Fig. 1A and B). The colon cancer dataset GSE39582 in the GEO database was selected for parallel verification. In GSE39582, 585 samples were divided into 443 tumor identification datasets, 123 tumor validation datasets, and 19 non-tumor datasets. The

findings demonstrated that PDCD11 expression in both the tumor identification dataset and the tumor validation dataset was higher than that in the non-tumor dataset, and the lack of significant difference particularly between the tumor identification and validation datasets was noteworthy (Fig. 1C and D; where C was probe 212422 and D was probe 212424). The lack of significant difference particularly in PDCD11 expression between the tumor identification and validation datasets was noteworthy (Fig. 1C and D; where C was probe 212422, and D was Probe 212424).

Utilizing data extracted from TCGA database, this investigation concentrated on the intricate landscape of PDCD11 expression across a spectrum of cancer types. Through precise analysis encompassing both paired and unpaired samples, it was discerned that within kidney chromophobe, PDCD11 expression exhibited a notable reduction in tumor tissues relative to their normal counterparts ($P < 0.05$). Conversely, a contrasting trend emerged in an array of malignancies, involving bladder urothelial carcinoma, invasive breast carcinoma, cholangiocarcinoma, colon adenocarcinoma, esophageal carcinoma, head and neck squamous cell carcinoma,
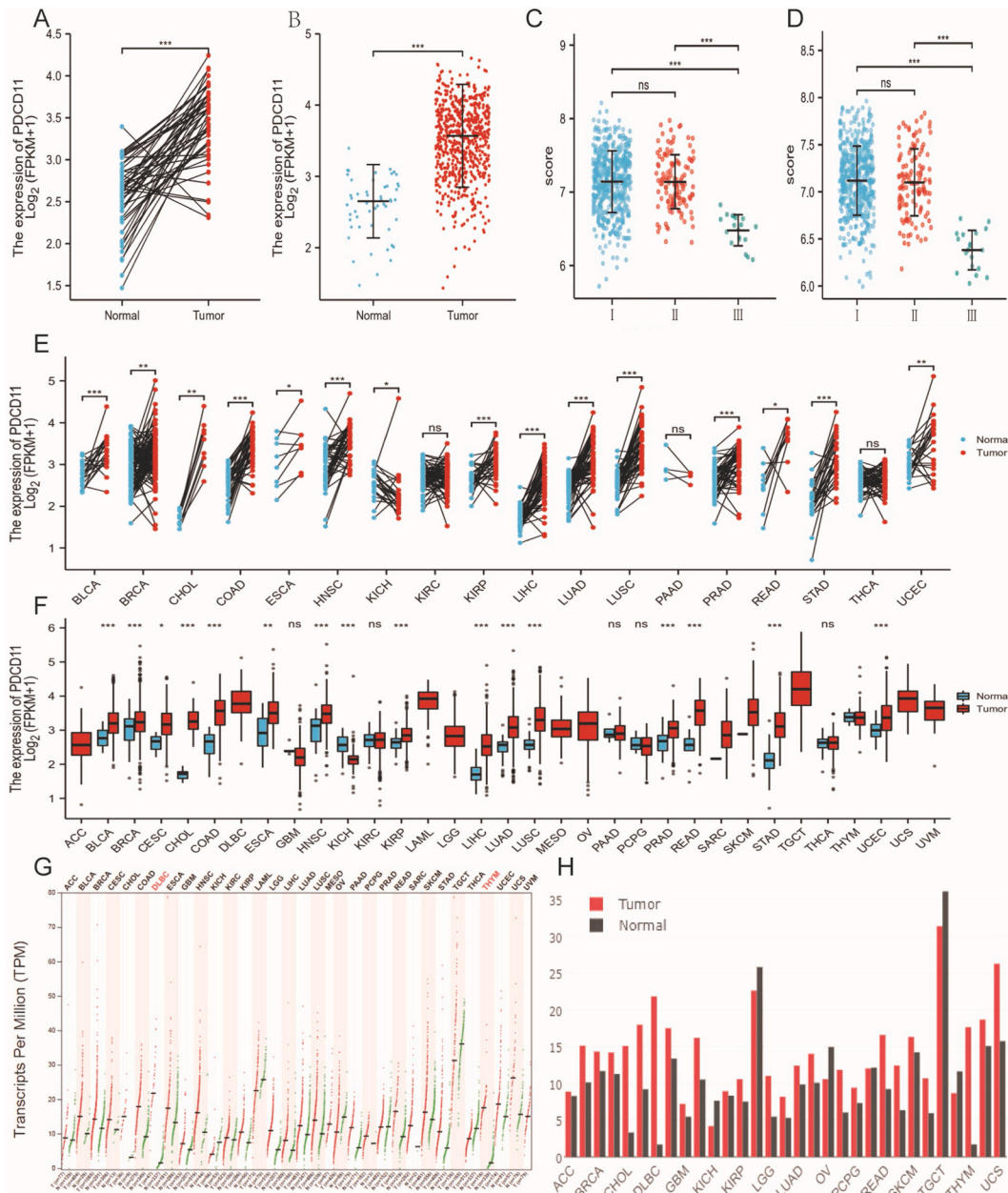

Fig. 1. PDCD11 expression in colorectal cancer and pan-cancer. A, PDCD11 expression in colorectal cancer paired samples. B, PDCD11 expression in colorectal cancer unpaired samples. C-D, PDCD11 expression in colon cancer GSE39582 dataset. E, PDCD11 expression in pan-cancer paired samples. F, PDCD11 expression in unpaired samples in pan-cancer. G-H, GEPIA database analysis of PDCD11 expression in pan-cancer, G marks the scatter diagram, and H marks the histogram.

papillary renal cell carcinoma, hepatocellular carcinoma, lung adenocarcinoma, lung squamous cell carcinoma, prostate adenocarcinoma, rectum adenocarcinoma, gastric adenocarcinoma, and uterine corpus endometrial carcinoma. In these cancer types, PDCD11 expression was significantly escalated within tumor tissues relative to their non-cancerous counterparts ($P < 0.05$) (Fig. 1E and F). It was suggested that PDCD11 might play a positive or negative role in different tumors, while in most tumors, it acts as a tumor-promoting molecule. In this study, the GEPIA database was utilized to undertake concurrent validation of PDCD11 expression in pan-cancer, yielding outcomes consistent with the aforementioned analysis (Fig. 1G and H).

3.2. Expression of PDCD11 RNA and protein in normal tissues and immunohistochemical results of normal tissues and tumor tissues

In this study, it was attempted to utilize the HPA database to quantify the mRNA and protein expression of PDCD11 in normal tissues, and the staining images of colon cancer tissues and normal tissues by immunohistochemical staining using two antibodies in the HPA database were displayed. The outcomes unveiled that PDCD11 mRNA and protein were expressed in most tissues, including the cerebral cortex, cerebellum, hippocampus, gallbladder, prostate, and bone marrow; there were obvious inconsistencies in mRNA and protein expression levels, suggesting that biological processes, such as post-transcriptional regulation or translational regulation, may be involved in these tissues (Fig. 2A and B). The immunohistochemical results of both antibodies also unveiled that the elevated PDCD11 expression in colon cancer tissues relative to para-carcinoma tissues (Fig. 2C–F).

Fig. 2. Analysis results of PDCD11 mRNA and protein expression in human normal tissues based on the HPA database and immunohistochemical results of colorectal cancer. A, mRNA expression of PDCD11 in human normal tissues. B, Protein expression of PDCD11 in human normal tissues. C–F, Immunohistochemical images of two PDCD11 antibodies in rectal and colon cancers from the HPA database.

3.3. The PPI network of PDCD11

PPI network of the interacting proteins of PDCD11 was established based on two databases. The GeneMANIA database analysis revealed a remarkable interaction profile for the top 20 proteins associated with PDCD11. Physical interactions dominated, constituting 77.64 % of the connections, followed by co-expression relationships at 8.01 %. Predicted interactions accounted for 5.37 %, while co-localization was responsible for 3.63 % of the associations. Genetic interactions contributed 2.87 %, pathway involvement comprised 1.88 %, and shared protein domains were the least represented at 0.60 % (Fig. 3A). The results of the STRING database showed the top 30 proteins interacting with PDCD11, with a total of 31 nodes and 462 lines (Fig. 3B).
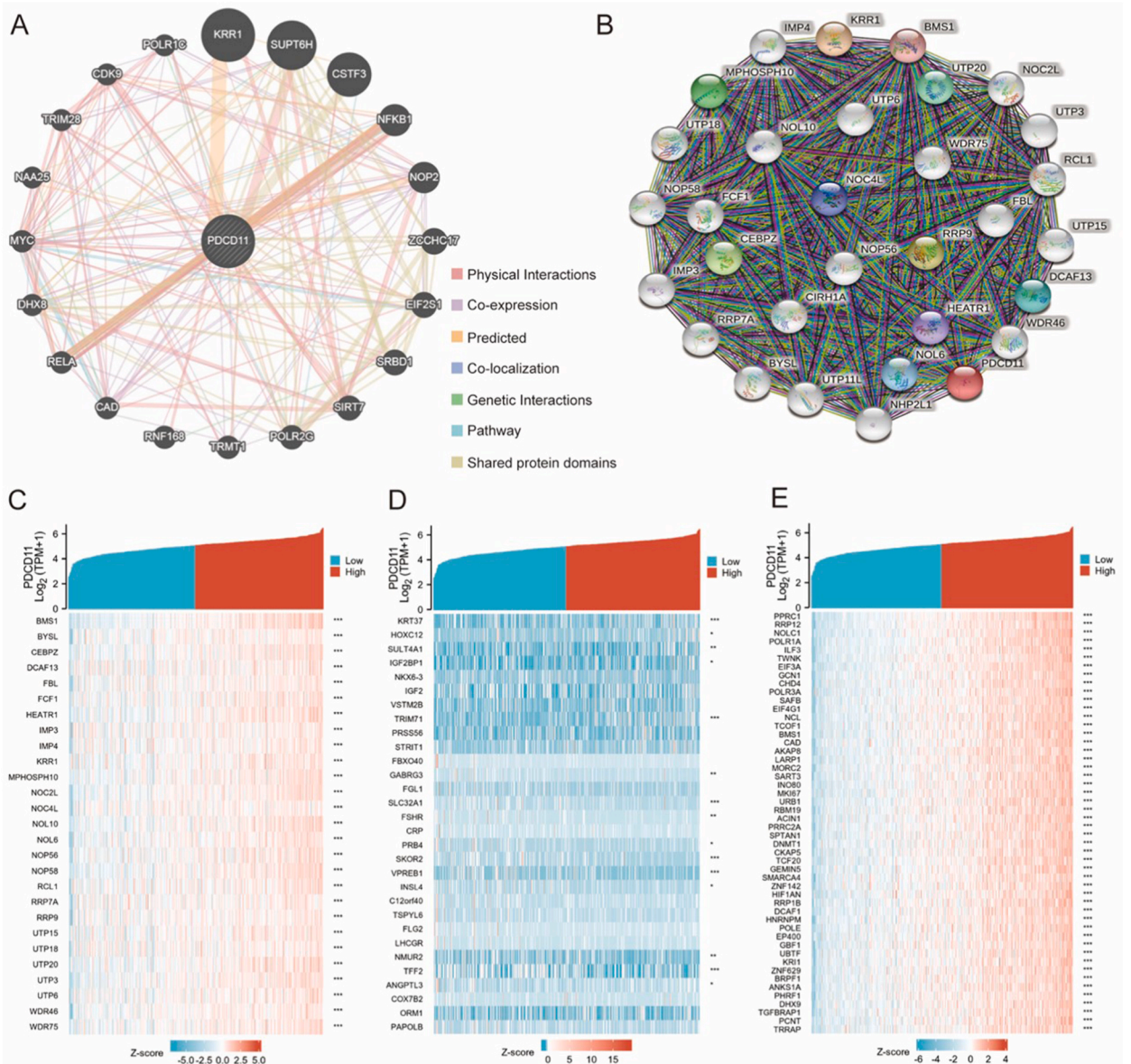
Fig. 3. The PPI of PDCD11, and PDCD11-related molecules screened based on the three strategies. A, PPI of PDCD11 was constructed based on the GeneMANIA database. B, PPI of PDCD11 was constructed based on the STRING database. C, PDCD11 co-A expression heat map was constructed based on the interaction molecules in the STRING database. D, The colorectal cancer data in the TCGA database were divided into high and low-expression groups based on the median expression level of PDCD11. After differential analysis, the differentially expressed molecules were screened out to construct the PDCD11 co-expression heat map. E, Co-expression heatmap was constructed after PDCD11-related molecules were screened out based on the colorectal cancer data in the TCGA database through molecular pairwise correlation analysis.

3.4. PDCD11-related molecules were screened based on three strategies

To investigate the biological activities of PDCD11 in colon cancer, three strategies were utilized to screen PDCD11-related molecules, and their correlations were displayed in a heat map. The top 30 proteins related to PDCD11 in the STRING database were screened, and correlation analysis was performed, which was displayed in the form of a correlation heat map (Fig. 3C). To elucidate the pathways impacted by varying expression levels of PDCD11 and to comprehend the biological functions of these pathways, the COAD (colon cancer) data attained from TCGA database were stratified into high and low expression groups on the basis of PDCD11 expression. The groups were compared, and the coding genes with Log FC > 1 and Log FC < −2 and adj.P < 0.05 were screened out and displayed by a correlation heat map (Fig. 3D). In this investigation, the relationship of PDCD11 with other molecules in colon cancer was unveiled through Pearson correlation analysis, leveraging data from TCGA database. By assessing correlation level, it was attempted to elucidate the biological processes influenced by PDCD11. Thereafter, a correlation heatmap delineating the top 50 coding genes was constructed to display the associations (Fig. 3E).

3.5. GO and KEGG enrichment analysis of PDCD11-related molecules

After the molecules related to PDCD11 were screened using the three strategies described above, GO and KEGG enrichment assays were implemented on these molecules, respectively, to find out which PDCD11-associated pathways could specifically affect and to evaluate the biological properties of these pathways.

The enrichment analysis outcomes of the 30 molecules screened from the STRING database elucidated intricate insights (Fig. 4A). The GO enrichment was examined across three hierarchical levels: biological process (BP), cellular component (CC), and molecular function (MF), adhering to stringent criteria of p. adj<0.1 and q value < 0.2. This comprehensive analysis unveiled a complex interplay
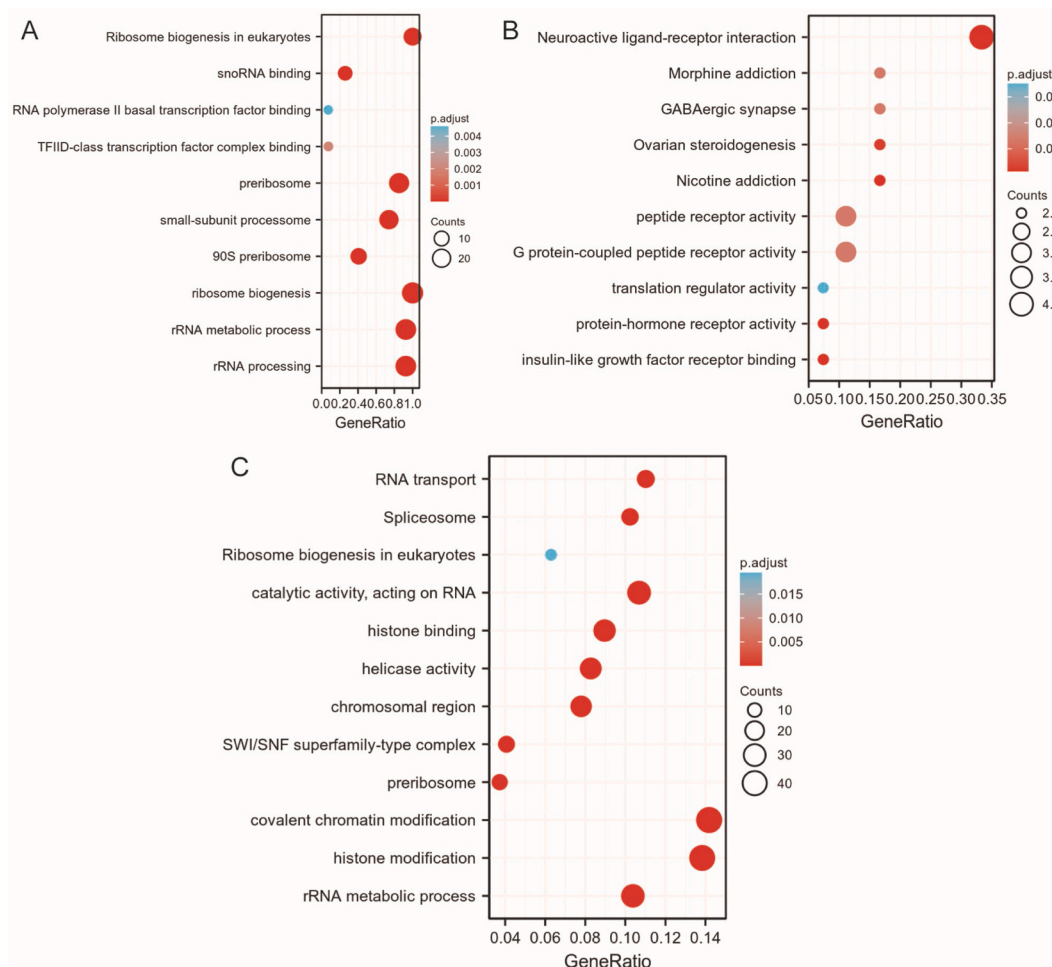

Fig. 4. GO and KEGG enrichment analysis of PDCD11-related molecules screened based on the three strategies. A, GO and KEGG enrichment analysis of the relevant molecules in the STRING database. B, GO and KEGG enrichment analysis of differentially expressed molecules. C, GO and KEGG enrichment analysis of related molecules revealed by correlation analysis.

of molecular functions and cellular localizations. Concurrently, the KEGG pathway analysis demonstrated an enrichment converging on a common pathway. The BPs enriched in the top three included ribosome biogenesis (GO: 0042254), rRNA processing (GO: 0006364), and rRNA metabolic process (GO: 0016072); the CCs enriched in the top three included preribosome (GO: 0030684), small-subunit processome (GO: 0032040), and 90S preribosome (GO: 0030686); the MFs enriched in the top three included snoRNA binding (GO: 0030515), TFIID-class transcription factor complex binding (GO: 0001094), and RNA polymerase II basal transcription factor binding (GO: 0001091). The pathway enriched by KEGG was ribosome biogenesis in eukaryotes (hsa03008).
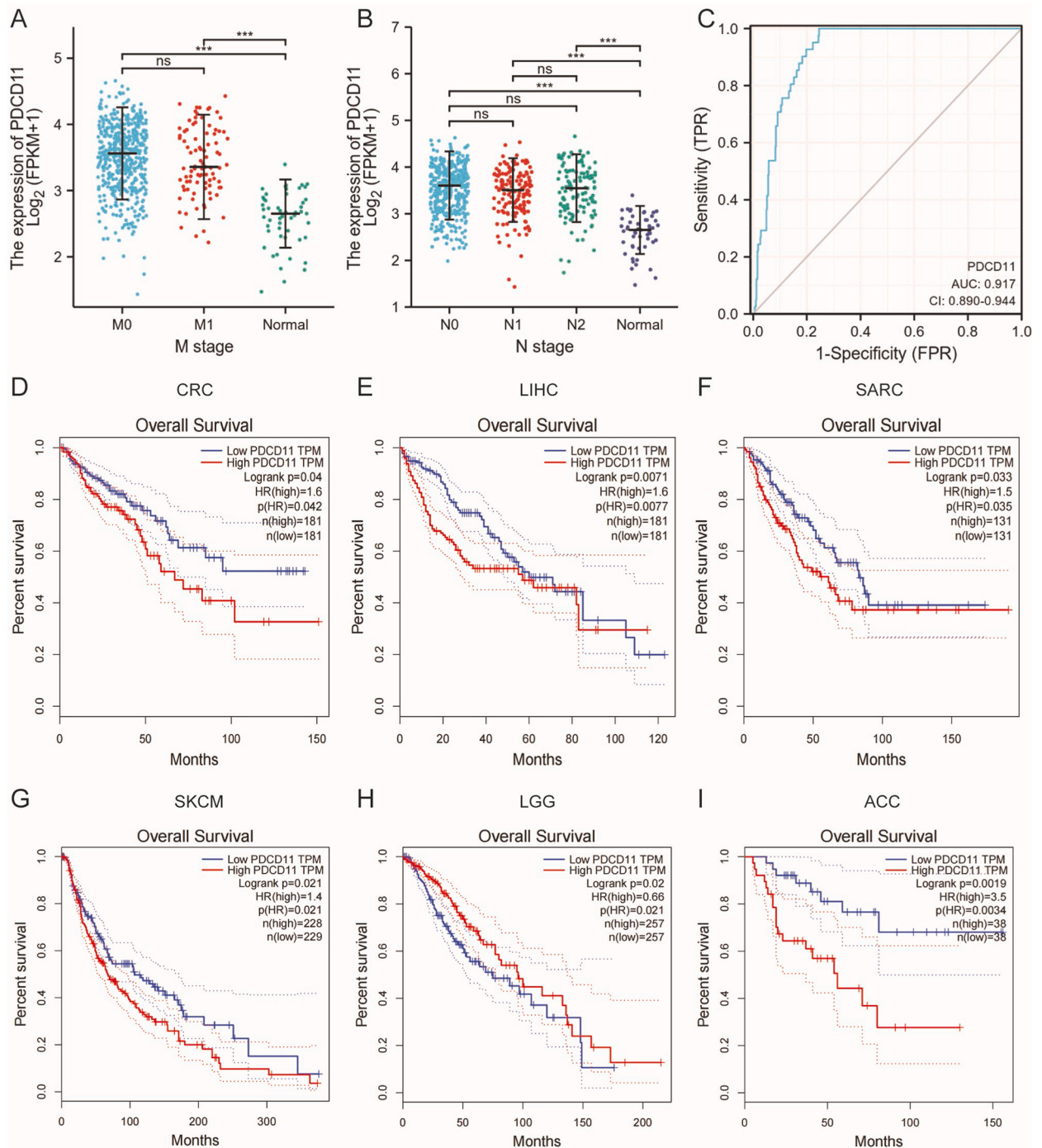
Fig. 5. Correlation analysis between PDCD11 expression and prognosis. A-B, Correlation of PDCD11 expression with N and M stages of colorectal cancer. C, ROC of PDCD11 as a predicting target molecule. D-E, Correlation analysis of PDCD11 expression with OS of CRC, LIHC, SARC, SKCM, ACC, and LGG.

The outcomes of the enrichment analysis of the 30 molecules, screened based on the differential analysis of PDCD11 expression, revealed significant findings (Fig. 4B). The GO enrichment analysis unveiled MF enrichment at a p. adj<0.1 and q value < 0.2. Additionally, the KEGG enrichment analysis identified six distinct pathways, further elucidating the molecular interactions influenced by PDCD11 expression. The top 5 functions in the MF were insulin-like growth factor receptor binding (GO: 0005159), protein-hormone receptor activity (GO: 0016500), G protein-coupled peptide receptor activity (GO: 0008528), peptide receptor activity (GO: 0001653), and translation regulator activity (GO: 0045182). The top five pathways enriched by KEGG were neuroactive ligand-receptor interaction (hsa04080), nicotine addiction (hsa05033), ovarian steroidogenesis (hsa04913), GABAergic synapse (hsa04727), and morphine addiction (hsa05032).

Based on the molecules indicated by PDCD11 correlation analysis, it was attempted to screen the top 300 molecules for GO and KEGG enrichment analysis. In the GO enrichment analysis results, the top 3 rankings of BP, CC, and MF were selected for illustration (p. adj<0.1 & q value < 0.2). The top 3 pathways were selected for displaying utilizing the KEGG enrichment analysis (p. adj<0.1 & q value < 0.2) (Fig. 4C). The BPs enriched in the first three were covalent chromatin modification (GO: 0016569), histone modification (GO: 0016570), and rRNA metabolic process (GO: 0016072); the CCs enriched in the first three were SWI/SNF superfamily-type complex (GO: 0070603), chromosomal region (GO: 0098687), and preribosome (GO: 0030684); the MFs enriched in the first three were histone binding (GO: 0042393), helicase activity (GO: 0004386), catalytic activity acting on RNA (GO: 0140098). The top three pathways enriched by KEGG were spliceosome (hsa03040), RNA transport (hsa03013), and ribosome biogenesis in eukaryotes (hsa03008).

3.6. Correlation analysis of PDCD11 expression with tumor prognosis

To figure out the potential prognostic significance of PDCD11 expression, a detailed analysis of its correlation with colon cancer stages was performed, alongside evaluating the receiver operating characteristic (ROC) curve to discern PDCD11's predictive capability as a tumor biomarker. Furthermore, it was attempted to figure out the relationship of PDCD11 expression with the prognosis of
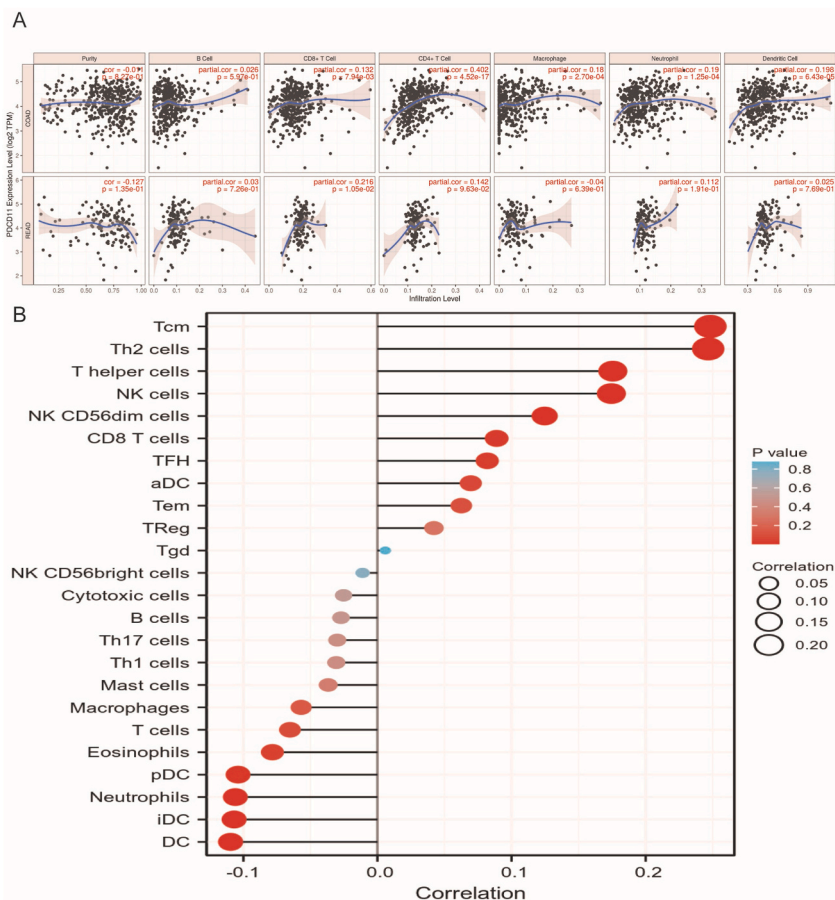

Fig. 6. Correlation analysis of PDCD11 expression and immune infiltration. A, The correlation between the expression of PDCD11 and the abundance of six immune cells in colorectal cancer was analyzed based on the TIMER database. B, The correlation between PDCD11 expression and 24 types of immune cells was analyzed by R software.

multiple tumor types. The outcomes demonstrated that elevated PDCD11 expression was specifically associated with the M and N stages of CRC; however, it did not exhibit a notable correlation with the progression within these stages. The ROC curve outcomes unveiled that the predictive ability of the variable PDCD11 had higher accuracy in predicting tumor and normal outcomes (AUC = 0.917, CI = 0.890–0.944) (Fig. 5A–C). Survival analysis unveiled that high PDCD11 expression resulted in decreased OS of CRC, hepatocellular carcinoma (HCC), sarcoma (SARC), skin melanoma (SKCM), adrenal cortical carcinoma (ACC), and prolonged OSS of low-grade glioma (LGG) ($P < 0.05$) (Fig. 5D–I).

3.7. Correlation analysis of PDCD11 expression with ICIN

To comprehensively elucidate the relationship of PDCD11 expression with ICIN, a multifaceted analytical approach was utilized. Initially, it was attempted to utilize the TIMER database to examine the correlation of PDCD11 expression with the abundance of six distinct immune cell types: CD4+ T cells, CD8+ T cells, B cells, neutrophils, DCs, and MACs. The assay revealed that in colon cancer, the significantly positive link of PDCD11 expression with the infiltration levels of neutrophils, DCs, and MACs, CD8+ T cells, and CD4+ T cells was noteworthy (P < 0.05). However, its significant correlation with B cells was not achieved (P > 0.05) (Fig. 6A).

Subsequently, leveraging data from TCGA database, it was attempted to implement an in-depth assay on the correlation of PDCD11 expression with 24 distinct immune cell types. The findings were graphically depicted through a lollipop chart, where the magnitude of each circle denotes the extent of correlation, in which larger circles signify a more remarkable correlation. The vertical position of each circle (distance from zero) is suggestive of the correlation strength, with positive values denoting a positive correlation and negative values reflecting a negative correlation. Additionally, the intensity of the circle's color corresponds to the P-value derived from the correlation statistics, with deeper hues representing higher statistical significance. The assay revealed that the positive association of PDCD11 expression with several immune cell types, including NK cells, T helper cells, Th2 cells, central memory T cells (Tcm), NK CD56dim cells, CD8+ T cells, and TFH. Conversely, it exhibited a negative correlation with DC, neutrophils, iDC, pDC, and eosinophils (Spearman correlation analysis, P < 0.05) (Fig. 6B).
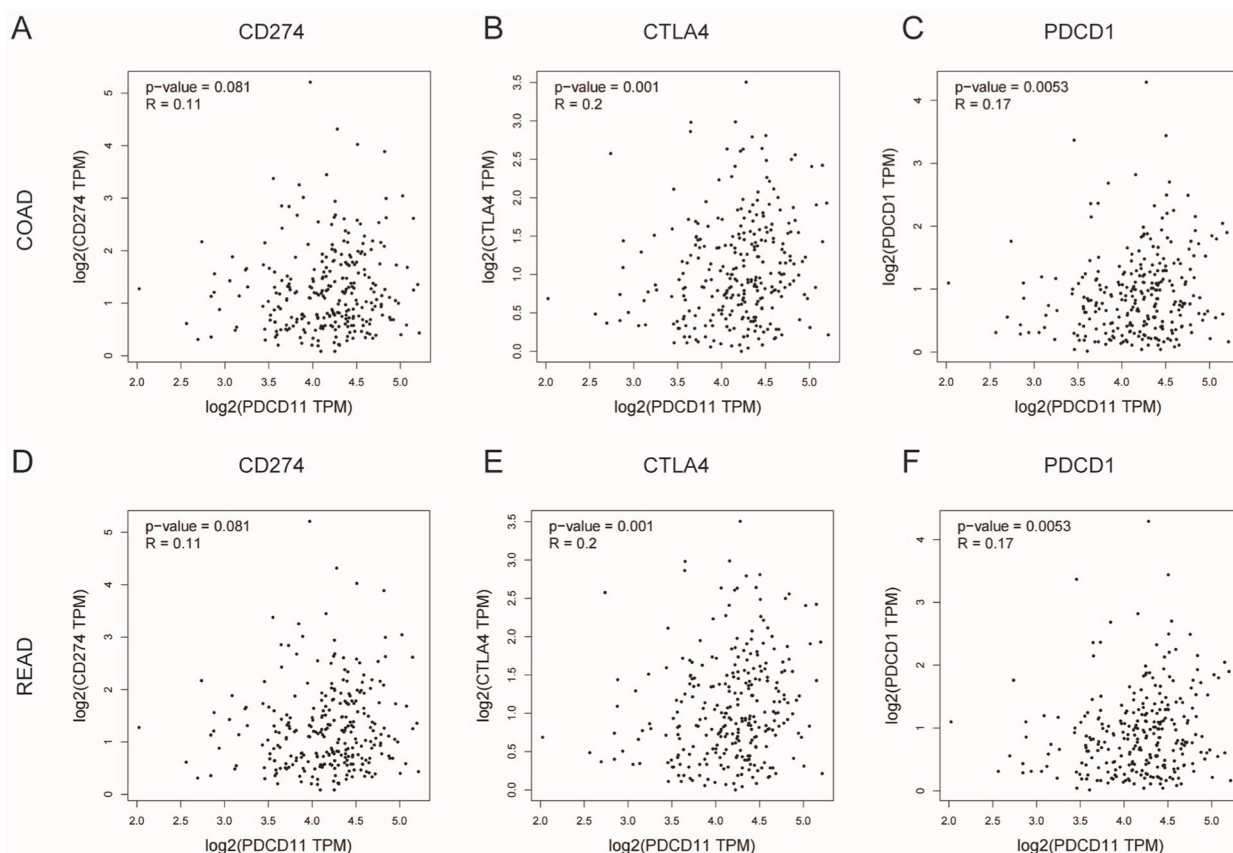

Fig. 7. A-F, Correlation analysis between PDCD11 expression in colorectal cancer and three common immune checkpoints in colon cancer by the GEPIA database.

3.8. Correlation of PDCD11 expression with three common colon cancer immune checkpoints

Since the expression levels of immune checkpoint-related genes were closely related to the response to immune checkpoint inhibitor therapy, the association of PDCD11 with three important immune checkpoints (ICKs) in the colon and rectal cancers, including PDCD1 (PD-1), CD274 (PD-L1), and CTLA-4, was evaluated. The interrelationship between PDCD11 and the immunoregulatory molecules PDCD1 (PD-1), CD274 (PD-L1), and CTLA-4 was elucidated through Pearson correlation analysis. The outcomes unveiled that in colon cancer and rectal cancer, PDCD11 expression was positively correlated with CTLA4 and PDCD11 ($P < 0.05$), rather than with CD274 (Fig. 7A–F).

3.9. Lentiviral transduction of PDCD11 shRNA in RKO cells

To investigate the function of PDCD11 in CRC, the knockdown effects of lentiviruses carrying PDCD11 shRNAs or scramble shRNA in RKO cells were evaluated. As illustrated in Fig. 8A, fluorescence microscopy revealed that the transduction efficiency of two GFP-containing PDCD11 shRNA lentiviruses (PSC47374 and PSC47375) in RKO cells following 72-h infection was both >80 %. Data from qRT-PCR revealed that the knockdown effect of PSC47374 lentiviruses in RKO cells was 71.1 % and that of PSC47375 was 80.4 % (Fig. 8B). The results of immunoblotting unveiled that two PDCD11 shRNA lentiviruses decreased the protein levels of PDCD11 in RKO cells (Fig. 8C and S. 1A). These data suggested that PDCD11 shRNA lentiviruses were successfully constructed.

3.10. Lentivirus-mediated PDCD11 knockdown inhibited RKO cell proliferation, colony formation, and migration while inducing the apoptosis

In this section, our concentration was on exploring the regulatory function of PDCD11 in CRC. When RKO cells were infected with PDCD11 shRNA lentiviruses or scramble shRNA lentivirus for 72 h, the Celigo image cytometry system was employed to detect RKO cell growth after transduction with PDCD11 shRNA lentiviruses or scramble shRNA lentivirus on days 1, 2, 3, 4, and 5 of incubation. As depicted in Fig. 9A–C, the number of fluorescent RKO cells with lentiviral transduction of two PDCD11 shRNAs was declined compared with cells transduced with scramble shRNA lentivirus. As expected, fewer colonies of RKO cells were observed upon lentiviral transduction of two PDCD11 shRNAs than transduction of scramble shRNA lentivirus (Fig. 9D–E). Accordingly, the MTT assay unveiled that PDCD11 knockdown by two PDCD11 shRNA lentiviruses inhibited RKO cell viability (Fig. 10A). Flow cytometry of annexin V-APC single staining revealed more apoptotic RKO cells upon lentiviral transduction of two PDCD11 shRNAs than transduction of scramble
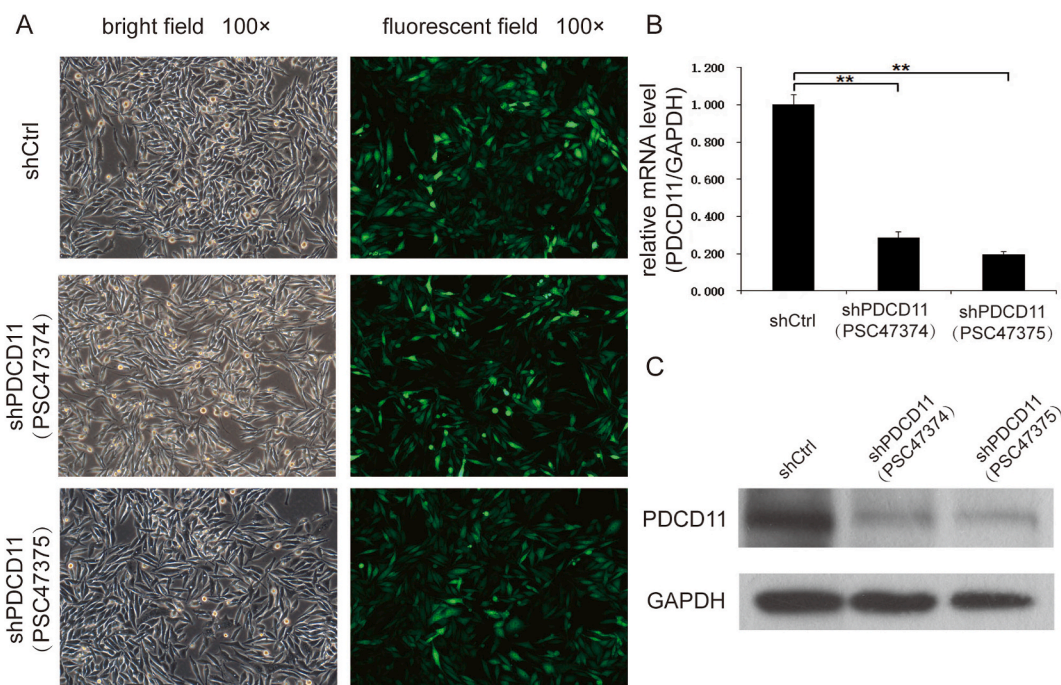

Fig. 8. Lentiviral transduction of PDCD11 shRNA in RKO cells. A, Fluorescence images (100 ×) of RKO cells after transduction with two GFP-containing PDCD11 shRNA lentiviruses (PSC47374 and PSC47375) or scramble shRNA for 72 h. B, mRNA expression levels of PDCD11 in RKO cells following lentiviral transduction of PDCD11 shRNAs or scramble shRNA were determined by qRT-PCR. C, Immunoblots of PDCD11 in RKO cells following lentiviral transduction of PDCD11 shRNAs or scramble shRNA. **$p < 0.01$. Each experiment was carried out in triplicate. Unpaired t-test was utilized for statistical comparison.
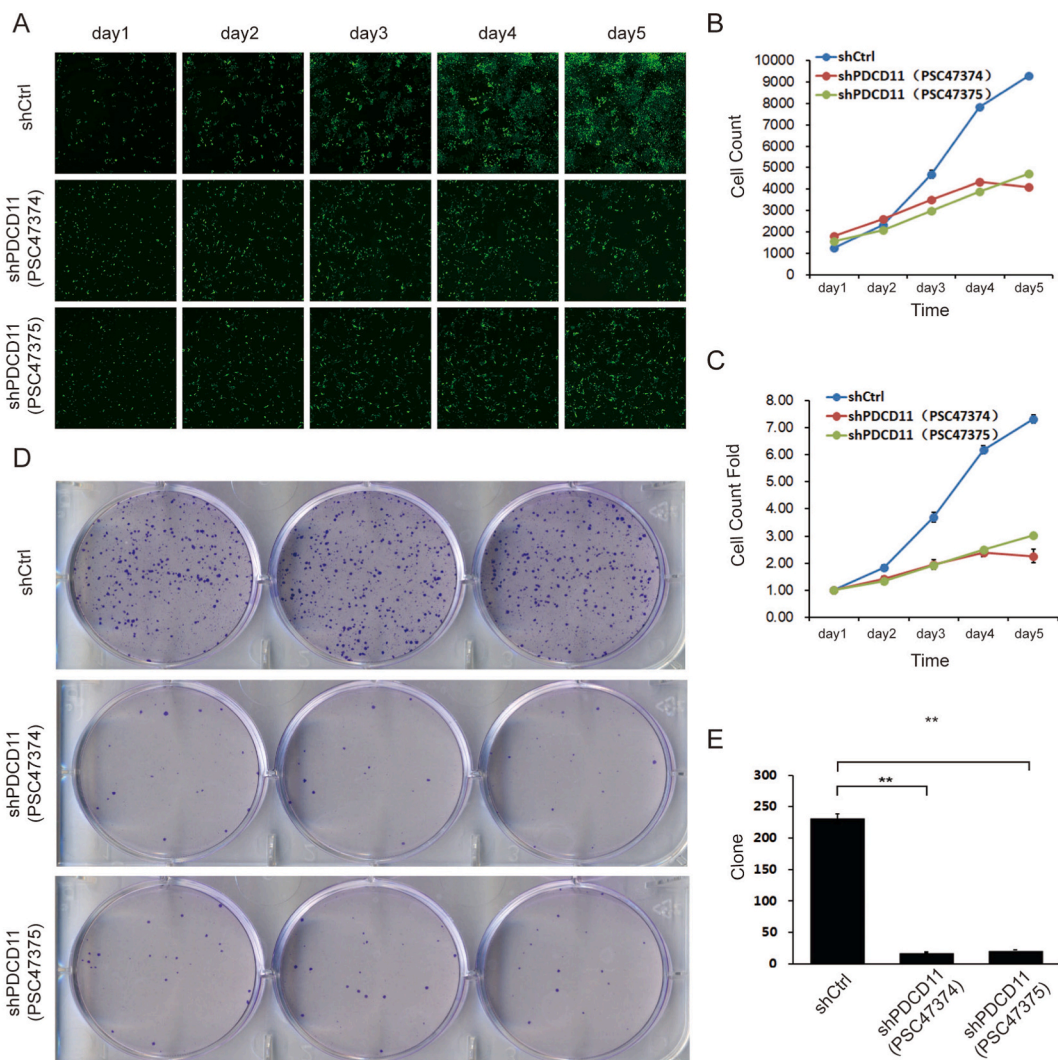
Fig. 9. Lentivirus-mediated PDCD11 knockdown inhibits RKO cell proliferation and colony formation. A, The number of fluorescent RKO cells with lentiviral transduction of two PDCD11 shRNAs or scramble shRNA was examined by Celigo image cytometry system on day 1, 2, 3, 4, and 5 of incubation. Repeated measurements ANOVA with Bonferroni corrections were utilized for statistical comparison. B, The number of colonies of RKO cells with lentiviral transduction of two PDCD11 shRNAs or scramble shRNA. Unpaired *t*-test was utilized for statistical comparison. **$p < 0.01$. Each experiment was carried out in triplicate.

shRNA lentivirus (Fig. 10B). Besides, wound healing assay plus the Celigo image cytometry and Transwell migration assay were concurrently performed to examine the effects of PDCD11 on RKO cell migration. The outcomes unveiled fewer fluorescent cells were found in the wound area (Fig. 11A–B), and fewer cells migrated from the upper chamber to the lower chamber (Fig. 11C–E) when RKO cells were infected with PDCD11 shRNA lentiviruses for 72 h compared with infection of scramble shRNA lentivirus. These data indicated that PDCD11 knockdown inhibited RKO cell proliferation, colony formation, and migration, whereas induced apoptosis.

4. Discussion

Despite the strides made in systemic therapies for advanced CRC, patients' prognosis in this group remains discouraging. This investigation unveiled a noticeable elevation in PDCD11 expression level in cancerous tissues relative to adjacent non-cancerous tissues, a trend evident in both paired and unpaired samples of colon cancer. The colon cancer dataset GSE39582 selected from the GEO database was used for parallel verification, and the same result was finally obtained, reflecting a greater PDCD11 expression in cancer tissues relative to para-carcinoma tissues. Additionally, it was also found that PDCD11 was highly expressed in other malignancies, except KICH (renal chromophobe carcinoma), which was lowly expressed. The above outcomes indicated that PDCD11 is likely to be a tumor-promoting molecule, thus affecting the prognosis of the disease. In contrast, evidence from cellular experiments showed that lentivirus-mediated PDCD11 knockdown inhibited CRC cell proliferation, colony formation, and migration while
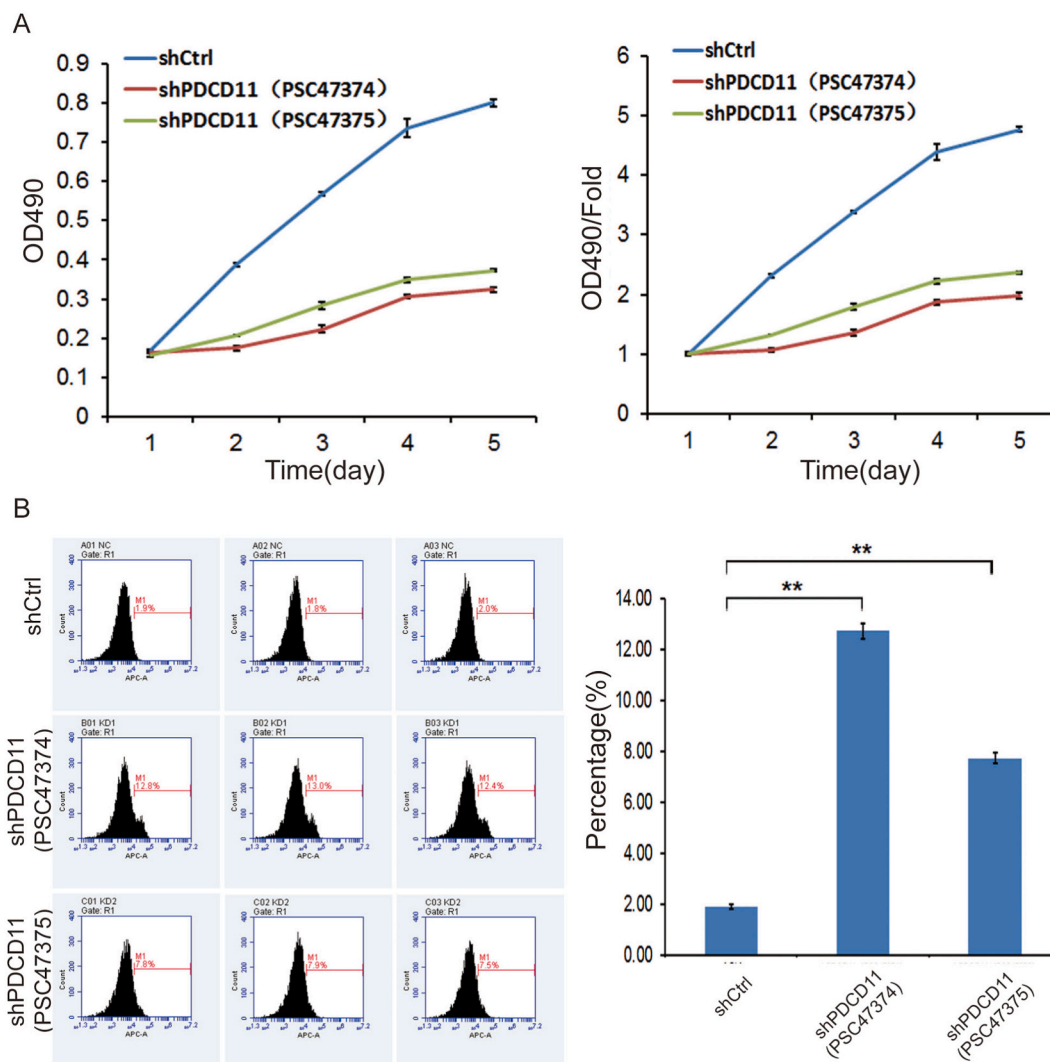
Fig. 10. Lentivirus-mediated PDCD11 knockdown inhibits RKO cell viability but induces cell apoptosis. A, The viability of RKO cells with lentiviral transduction of two PDCD11 shRNAs or scramble shRNA was examined by MTT assay on day 1, 2, 3, 4, and 5 of incubation. Repeated measurements ANOVA with Bonferroni corrections were utilized for statistical comparison. B, Flow cytometric analysis of annexin V-APC single staining detected apoptotic RKO cells following lentiviral transduction of two PDCD11 shRNAs or scramble shRNA. Unpaired t-test was utilized for statistical comparison. *$p < 0.05$, compared with two shPDCD11.Each experiment was carried out in triplicate.

inducing apoptosis, suggesting that PDCD11 might play an oncogenic function in CRC.

Prior research [31] indicated that PDCD11 has the capability to modulate the G2/M checkpoint by influencing the p53-CDK1 and CDC25/CCDK1 signaling pathways. This positioning within cell-cycle networks indicates that PDCD11 might serve as a crucial hub and a potential target for CRC therapy. Notably, PDCD11 does not directly intervene in the regulation of p53 transcription factor level or activity. Instead, it may play a noticeable function in counteracting apoptosis triggered by DNA damage stress, particularly in a manner contingent upon p53's involvement. Studies [32–34] recently concluded that PDCD11's anti-apoptotic effects might be modulated through its influence on post-translational modifications of p53 or its intricate interactions with other molecular entities, pathways that can modulate apoptosis independently of p53's transcriptional actions. Given the paramount importance of dysfunctional DNA damage response (DDR) pathways in hampering the efficacy of chemotherapy, in the landscape of CRC management, therapeutic interventions aimed at modulating DDR pathways are noteworthy [35–38]. By inhibiting PDCD11, it might be possible to sensitize CRC cells to DDR signals, thereby potentially enhancing the therapeutic responsiveness to chemotherapy [31]. The outcomes of the present investigation unveiled that the high expression of PDCD11 was only related to M and N stages in CRC, and unassociated with the progression of M and N stages. The ROC outcomes unveiled that the predictive ability of PDCD11 had high accuracy in predicting tumor or normal tissues, and survival analysis unveiled that the high expression of PDCD11 shortened OS of CRC, HCC, SARC, SKCM, and ACC. In order to clarify the correlation of PDCD11 with ICIN, different databases were utilized. The data attained from the TIMER database unveiled that in the context of colon cancer, PDCD11 expression exhibited a positive correlation with a range
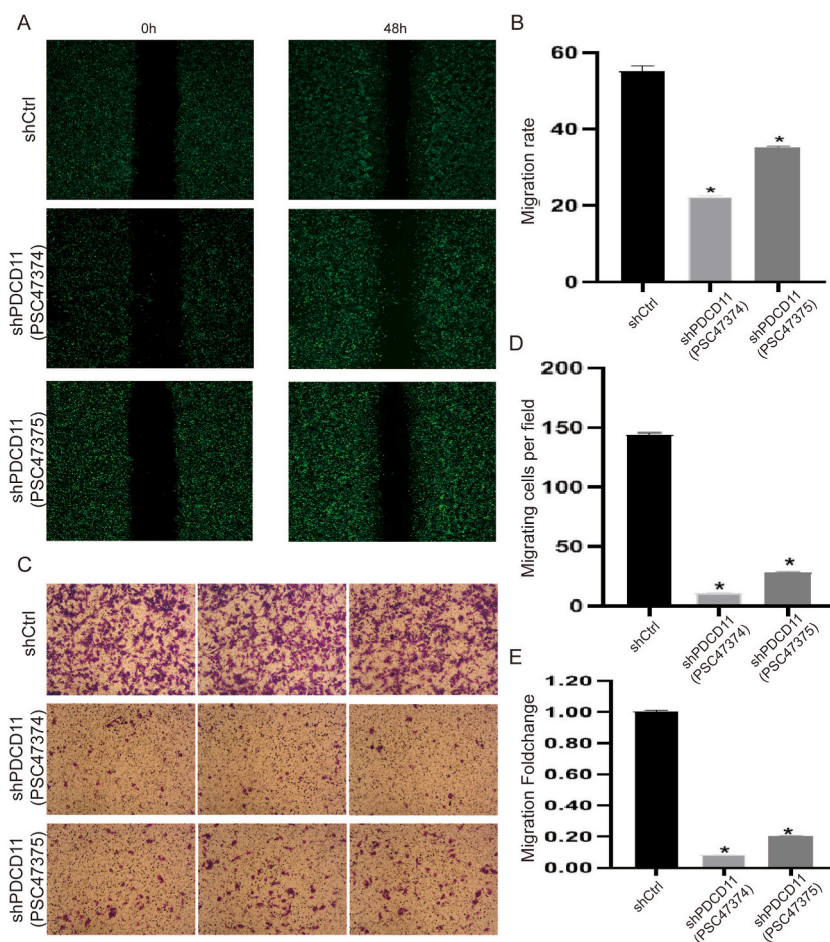
Fig. 11. Lentivirus-mediated PDCD11 knockdown inhibits RKO cell migration. A, Celigo Image Cytometer was used to detect fluorescent RKO cells in the wound area from 0 h to 48 h after incubation with serum-free DMEM, when RKO cells were infected with PDCD11 shRNA lentiviruses or scramble shRNA lentivirus for 72 h. B, The migration of RKO cells with lentiviral transduction of two PDCD11 shRNAs or scramble shRNA was analyzed by Transwell assay without Matrigel. Unpaired *t*-test was utilized for statistical comparison. *$p < 0.05$, compared with two shPDCD11.Each experiment was carried out in triplicate.

of immune cells, including neutrophils, DCs, CD8$^+$ T cells, CD4$^+$ T cells, and MACs. This reflects a potential function of PDCD11 in modulating the tumor immune microenvironment by enhancing the presence of these immune cell types. Conversely, data from TCGA database demonstrated that PDCD11 expression could be positively linked with NK cells, T helper cells, Th2 cells, Tcm, CD56dim NK cells, CD8$^+$ T cells, and TFH. In contrast, the negative link of PDCD11 expression with DCs, neutrophils, iDCs, pDCs, and eosinophils was noteworthy. These results above verified our hypothesis to a certain extent that the high PDCD11 expression could influence cancerous cases' prognosis and is linked to the ICIN of tumors (e.g., CRC). ICIs have become first-line drugs for a variety of malignancies, and immunotherapy, surgery, chemotherapy, radiotherapy, and cancer-targeted therapy are considered equally important [39]. PDCD11 is likely to become a target molecule, similar to PD-1, for the therapy of CRC and other tumors, and its inhibitor will be developed against its ICIN properties to benefit CRC patients.

We acknowledge the contrasting outcomes between our bioinformatic analysis and cellular experiments. The bioinformatic analysis, utilizing the CRC GSE39582 dataset, suggested a potential association between high PDCD11 expression and tumor progression. On the other hand, cellular experiments demonstrated that PDCD11 knockdown inhibited CRC cell proliferation and induced apoptosis, indicating an oncogenic function of PDCD11. This discrepancy could be attributed to the complexity of tumor biology and the limitations of *in silico* predictions versus *in vitro* experiments. To reconcile these differences, consideration of the inherent limitations of both approaches is essential. Bioinformatic analyses rely on large-scale data from patient samples, which may encompass various stages and subtypes of CRC. These analyses provide valuable insights into potential molecular pathways and correlations, while do not account for the dynamic nature of tumor biology in a controlled setting. On the other hand, cellular experiments allow for targeted manipulation of specific genes or pathways in controlled environments, providing detailed mechanistic insights. However, these experiments mainly utilize cell lines that may not fully recapitulate the complexity of the tumor microenvironment. The observed discrepancy between bioinformatic analysis and cellular experiments underscores the necessity of integrative approaches in cancer

research. Future studies should aim to combine computational analyses with experimental validations to gain a comprehensive understanding of PDCD11's role in CRC. Techniques, such as patient-derived organoids or xenograft models can be employed to better mimic the tumor microenvironment and validate the effects of PDCD11 modulation on tumor behaviors.

The findings of this study hold potential implications for identifying molecular pathways and potential therapeutic targets in CRC treatment. The elevated expression of PDCD11 in CRC tissues, along with its demonstrated oncogenic role in promoting cell proliferation, colony formation, and migration, highlights the significance of this molecule in CRC pathogenesis. Further investigation into the specific mechanisms by which PDCD11 influences these processes will uncover novel molecular pathways crucial for CRC development. Moreover, the positive correlation of PDCD11 expression with ICIN in colon cancer suggests a complex interplay between PDCD11 and the immune microenvironment. Targeting PDCD11 could not only inhibit its tumor-promoting effects, but also modulate immune cell interactions, presenting a dual therapeutic opportunity. Regarding cancer treatment, ICIs have revolutionized therapy for various malignancies. Considering the positive correlation of PDCD11 expression with ICIN, similar to immune checkpoint molecules, PDCD11 inhibitors might serve as a promising candidate for immunotherapy. By targeting PDCD11, it may be possible to enhance immune responses against CRC cells, leading to the improved treatment outcomes. These findings suggest that PDCD11 could be a potential therapeutic target in CRC, and its inhibition may provide a dual benefit by both impeding tumor progression and enhancing anti-tumor immune responses. Further elucidation of the specific molecular pathways influenced by PDCD11 and its interactions with the immune system may promote the development of targeted therapies for CRC patients.

Although we investigated the expression of PDCD11 in CRC, along with its correlation with prognosis and ICIN, and confirmed through cellular experiments that PDCD11 promotes colon carcinogenesis and development by enhancing proliferation, invasive metastasis, and anti-apoptosis of colon cancer cells, we did not discuss the specific mechanisms involved in this study. This aspect will be thoroughly explored in subsequent research to provide a deeper understanding.

As a member of the programmed protein family, limited research was performed on PDCD11. However, through bioinformatics analysis, we conducted in-depth mining on CRC datasets that had been uploaded to public databases and analyzed genetic epigenetics, tumor stage, prognosis, and ICIN of CRC. The outcomes confirmed that PDCD11 is involved in the onset and progression of CRC, affects the prognosis of CRC and other tumors, and is correlated with the ICIN of CRC. It is expected to further clarify the target of PDCD11 at CRC and other tumors through whole-genome sequencing and other genetic analysis technologies and provide the pre-clinical theoretical basis for risk assessment, early diagnosis, and immunosuppressive therapy of CRC.

Ethics statement

A local ethics committee attempted to authorize the study.

Funding

Consent for publication

Not Applicable.

Data availability statement

The corresponding author can supply datasets utilized in this investigation relying on request.

CRediT authorship contribution statement

Xiongfeng Li: Writing – original draft, Visualization, Methodology, Investigation, Formal analysis, Data curation. **Gaowa Sharen:** Writing – original draft, Visualization, Methodology, Investigation, Formal analysis, Data curation. **Minjie Zhang:** Writing – original draft, Visualization, Methodology, Investigation, Formal analysis, Data curation. **Lei Zhang:** Methodology, Investigation, Formal analysis, Data curation. **Kejian Liu:** Methodology, Investigation, Formal analysis, Data curation. **Yu Wang:** Methodology, Investigation, Formal analysis, Data curation. **Haidong Cheng:** Writing – review & editing, Supervision, Project administration, Methodology, Funding acquisition, Data curation, Conceptualization. **Mingxing Hou:** Writing – review & editing, Supervision, Project administration, Methodology, Funding acquisition, Data curation, Conceptualization.

Declaration of competing interest

The authors declare that they have no known competing financial interests or personal relationships that could have appeared to influence the work reported in this paper.

Acknowledgements

We thank Huilian Fan for participating in the data collation for this study.

Appendix A. Supplementary data

Supplementary data to this article can be found online at https://doi.org/10.1016/j.heliyon.2024.e35002.

References

[1] H. Sung, J. Ferlay, R.L. Siegel, M. Laversanne, I. Soerjomataram, A. Jemal, F. Bray, Global cancer statistics 2020: GLOBOCAN estimates of incidence and mortality worldwide for 36 cancers in 185 countries, CA Cancer J Clin 71 (3) (2021 May) 209–249, https://doi.org/10.3322/caac.21660.

[2] Y. Su, H.R. Zhan, X. Sun, R. Chen, L. Sun, J.J. Hao, X.P. Zhang, Y. Tian, R. Chen, Global guidelines of colorectal cancer screening in high-risk population with family history of colorectal cancer: a systematic review, Zhonghua Liuxingbingxue Zazhi 43 (9) (2022 Sep 10) 1469–1478, https://doi.org/10.3760/cma.j.cn112338-20220422-00331.

[3] C.J. Yang, L. Zhao, Y.L. Lin, Y.J. Ye, S. Wang, Z.L. Shen, Advances in immune microenvironment and immunotherapy strategy for colorectal cancer, Journal of Colorectal & Anal Surgery 28 (4) (2022) 311–316, https://doi.org/10.19668/j.cnki.issn1674-0491.2022.04.001.

[4] Y. Ren, X. Chen, K.D. Chen, A.X. Ma, Economic burden of colorectal cancer in China: a systematic review, China Journal of Pharmaceutical Economics 17 (7) (2022) 5–11.

[5] J.F. Qiu, The Function and Mechanism of FOXS1 in Invasion and Metastasis of Colorectal Cancer [dissertation]. Guangzhou (GD), Southern Medical University, 2020.

[6] E. Lacana, L. D'Adamio, Regulation of Fas ligand expression and cell death by apoptosis-linked gene 4, Nat. Med. 5 (5) (1999 May) 542–547, https://doi.org/10.1038/8420.

[7] N. Perebaskine, S. Thore, S. Fribourg, Structural and interaction analysis of the Rrp5 C-terminal region, FEBS Open Bio 8 (2018) 1605–1614.

[8] T. Sweet, W. Yen, K. Khalili, S. Amini, Evidence for involvement of NFBP in processing of ribosomal RNA, J. Cell. Physiol. 214 (2008) 381–388.

[9] A.J. Turner, A.A. Knox, J.L. Prieto, B. McStay, N.J. Watkins, A novel small-subunit processome assembly intermediate that contains the U3 snoRNP, nucleolin, RRP5, and DBP4, Mol. Cell Biol. 29 (2009) 3007–3017.

[10] W. Eid, D. Hess, C. Konig, C. Gentili, S. Ferrari, The human Exonuclease-1 interactome and phosphorylation sites, Biochem. Biophys. Res. Commun. 514 (2019) 567–573.

[11] S. Lebaron, A. Segerstolpe, S.L. French, T. Dudnakova, F. de Lima Alves, S. Granneman, et al., Rrp5 binding at multiple sites coordinates pre-rRNA processing and assembly, Mol Cell. 52 (2013) 707–719.

[12] S. Khoshnevis, I. Askenasy, M.C. Johnson, M.D. Dattolo, C.L. Young-Erdos, M.E. Stroupe, et al., The DEAD-box protein Rok1 orchestrates 40S and 60S ribosome assembly by promoting the release of Rrp5 from Pre-40S ribosomes to allow for 60S maturation, PLoS Biol. 14 (2016) e1002480.

[13] R. Yang, M. Zhan, M. Guo, H. Yuan, Y. Wang, Y. Zhang, et al., Yolk sac-derived Pdcd11-positive cells modulate zebrafish microglia differentiation through the NFkappaB-Tgfbeta1 pathway, Cell Death Differ. 28 (2021) 170–183.

[14] R. Yang, M. Zhan, M. Guo, H. Yuan, Y. Wang, Y. Zhang, W. Zhang, S. Chen, H. de The, Z. Chen, J. Zhou, J. Zhu, Yolk sac-derived Pdcd11-positive cells modulate zebrafish microglia differentiation through the NF-κB-Tgfβ1 pathway, Cell Death Differ. 28 (1) (2021 Jan) 170–183, https://doi.org/10.1038/s41418-020-0591-3.

[15] A. Castro, R.M. Pyke, X. Zhang, W.K. Thompson, C.P. Day, L.B. Alexandrov, M. Zanetti, H. Carter, Strength of immune selection in tumors varies with sex and age, Nat. Commun. 11 (1) (2020 Aug 17) 4128, https://doi.org/10.1038/s41467-020-17981-0.

[16] S. Hamarsheh, O. Groß, T. Brummer, R. Zeiser, Immune modulatory effects of oncogenic KRAS in cancer, Nat. Commun. 11 (1) (2020 Oct 28) 5439, https://doi.org/10.1038/s41467-020-19288-6.

[17] B. Benner, L. Scarberry, L.P. Suarez-Kelly, M.C. Duggan, A.R. Campbell, E. Smith, G. Lapurga, K. Jiang, J.P. Butchar, S. Tridandapani, J.H. Howard, R.A. Baiocchi, T.A. Mace, W.E. Carson 3rd, Generation of monocyte-derived tumor-associated macrophages using tumor-conditioned media provides a novel method to study tumor-associated macrophages in vitro, J Immunother Cancer 7 (1) (2019 May 28) 140, https://doi.org/10.1186/s40425-019-0622-0.

[18] A. Steven, B. Seliger, The role of immune escape and immune cell infiltration in breast cancer, Breast Car 13 (1) (2018 Mar) 16–21, https://doi.org/10.1159/000486585.

[19] M. Sade-Feldman, K. Yizhak, S.L. Bjorgaard, J.P. Ray, C.G. de Boer, R.W. Jenkins, D.J. Lieb, J.H. Chen, D.T. Frederick, M. Barzily-Rokni, S.S. Freeman, A. Reuben, P.J. Hoover, A.C. Villani, E. Ivanova, A. Portell, P.H. Lizotte, A.R. Aref, J.P. Eliane, M.R. Hammond, H. Vitzthum, S.M. Blackmon, B. Li, V. Gopalakrishnan, S.M. Reddy, Z.A. Cooper, C.P. Paweletz, D.A. Barbie, A. Stemmer-Rachamimov, K.T. Flaherty, J.A. Wargo, G.M. Boland, R.J. Sullivan, G. Getz, N. Hacohen, Defining T cell states associated with response to checkpoint immunotherapy in melanoma, Cell 175 (4) (2018 Nov 1) 998–1013.e20, https://doi.org/10.1016/j.cell.2018.10.038.

[20] D.F. McDermott, M.A. Huseni, M.B. Atkins, R.J. Motzer, B.I. Rini, B. Escudier, L. Fong, R.W. Joseph, S.K. Pal, J.A. Reeves, M. Sznol, J. Hainsworth, W.K. Rathmell, W.M. Stadler, T. Hutson, M.E. Gore, A. Ravaud, S. Bracarda, C. Suárez, R. Danielli, V. Gruenwald, T.K. Choueiri, D. Nickles, S. Jhunjhunwala, E. Piault-Louis, A. Thobhani, J. Qiu, D.S. Chen, P.S. Hegde, C. Schiff, G.D. Fine, T. Powles, Clinical activity and molecular correlates of response to atezolizumab alone or in combination with bevacizumab versus sunitinib in renal cell carcinoma, Nat. Med. 24 (6) (2018 Jun) 749–757, https://doi.org/10.1038/s41591-018-0053-3.

[21] B. Li, E. Severson, J.C. Pignon, H. Zhao, T. Li, J. Novak, P. Jiang, H. Shen, J.C. Aster, S. Rodig, S. Signoretti, J.S. Liu, X.S. Liu, Comprehensive analyses of tumor immunity: implications for cancer immunotherapy, Genome Biol. 17 (1) (2016 Aug 22) 174, https://doi.org/10.1186/s13059-016-1028-7.

[22] D. Bruni, H.K. Angell, J. Galon, The immune contexture and Immunoscore in cancer prognosis and therapeutic efficacy, Nat. Rev. Cancer. 20 (11) (2020 Nov 6) 626–680, https://doi.org/10.1038/s41568-020-0285-7.

[23] Z. Payandeh, S. Khalili, M.H. Somi, M. Mard-Soltani, A. Baghbanzadeh, K. Hajiasgharzadeh, N. Samadi, PD-1/PD-L1-dependent immune response in colorectal cancer, J. Cell. Physiol. 235 (7–8) (2020 Jul) 5461–5475, https://doi.org/10.1002/jcp.29494.

[24] Z. Tang, C. Li, B. Kang, G. Gao, C. Li, Z. Zhang, GEPIA: a web server for cancer and normal gene expression profiling and interactive analyses, Nucleic Acids Res. 45 (W1) (2017 Jul 3) W98–W102, https://doi.org/10.1093/nar/gkx247.

[25] G. Yu, L.G. Wang, Y. Han, Q.Y. He, clusterProfiler: an R package for comparing biological themes among gene clusters, OMICS 16 (5) (2012 May) 284–287, https://doi.org/10.1089/omi.2011.0118.

[26] B. Li, E. Severson, J.C. Pignon, H. Zhao, T. Li, J. Novak, P. Jiang, H. Shen, J.C. Aster, S. Rodig, S. Signoretti, J.S. Liu, X.S. Liu, Comprehensive analyses of tumor immunity: implications for cancer immunotherapy, Genome Biol. 17 (1) (2016 Aug 22) 174, https://doi.org/10.1186/s13059-016-1028-7.

[27] T. Li, J. Fan, B. Wang, N. Traugh, Q. Chen, J.S. Liu, B. Li, X.S. Liu, TIMER: a web server for comprehensive analysis of tumor-infiltrating immune cells, Cancer Res. 77 (21) (2017 Nov 1) e108–e110, https://doi.org/10.1158/0008-5472.CAN-17-0307.

[28] J. Racle, K. de Jonge, P. Baumgaertner, D.E. Speiser, D. Gfeller, Simultaneous enumeration of cancer and immune cell types from bulk tumor gene expression data, Elife 6 (2017 Nov 13) e26476, https://doi.org/10.7554/eLife.26476.

[29] G. Bindea, B. Mlecnik, M. Tosolini, A. Kirilovsky, M. Waldner, A.C. Obenauf, H. Angell, T. Fredriksen, L. Lafontaine, A. Berger, P. Bruneval, W.H. Fridman, C. Becker, F. Pagès, M.R. Speicher, Z. Trajanoski, J. Galon, Spatiotemporal dynamics of intratumoral immune cells reveal the immune landscape in human cancer, Immunity 39 (4) (2013 Oct 17) 782–795, https://doi.org/10.1016/j.immuni.2013.10.003.

[30] S. Hänzelmann, R. Castelo, J. Guinney, GSVA: gene set variation analysis for microarray and RNA-seq data, BMC Bioinf. 14 (2013 Jan 16) 7, https://doi.org/10.1186/1471-2105-14-7.

[31] L. Ding, Y. Xu, L. Xu, et al., Programmed cell death 11 modulates but not entirely relies on p53-HDM2 loop to facilitate G2/M transition in colorectal cancer cells, Oncogenesis 12 (1) (2023) 57.

[32] C. Castrogiovanni, B. Waterschoot, O. De Backer, P. Dumont, Serine 392 phosphorylation modulates p53 mitochondrial translocation and transcription-independent apoptosis, Cell Death Differ 25 (2018) 190–203.

[33] H. Arai, A. Elliott, J. Xiu, J. Wang, F. Battaglin, N. Kawanishi, et al., The landscape of alterations in DNA damage response pathways in colorectal cancer, Clin. Cancer Res. 27 (2021) 3234–3242.

[34] F. Catalano, R. Borea, S. Puglisi, A. Boutros, A. Gandini, M. Cremante, et al., Targeting the DNA damage response pathway as a novel therapeutic strategy in colorectal cancer, Cancers 14 (2022) 1388.

[35] S. Meršaková, Z. Lasabová, J. Strnádel, M. Kalman, E. Gabonova, P. Sabaka, R. Ciccocioppo, L. Rodrigo, P. Kruzliak, P. Mikolajčík, Genomic profile and immune contexture in colorectal cancer-relevance for prognosis and immunotherapy, Clin. Exp. Med. 21 (2) (2021) 195–204, https://doi.org/10.1007/s10238-020-00649-w.

[36] D. Bruni, H.K. Angell, J. Galon, The immune contexture and Immunoscore in cancer prognosis and therapeutic efficacy, Nat. Rev. Cancer. 20 (11) (2020 Nov) 662–680, https://doi.org/10.1038/s41568-020-0285-7.

[37] Z. Payandeh, S. Khalili, M.H. Somi, M. Mard-Soltani, A. Baghbanzadeh, K. Hajiasgharzadeh, N. Samadi, PD-1/PD-L1-dependent immune response in colorectal cancer, J. Cell. Physiol. 235 (7–8) (2020 Jul) 5461–5475, https://doi.org/10.1002/jcp.29494.

[38] A. Ooki, E. Shinozaki, K. Yamaguchi, Immunotherapy in colorectal cancer: current and future strategies, J. Anus. Rectum Colon. 5 (1) (2021 Jan 28) 11–24, https://doi.org/10.23922/jarc.2020-064.

[39] X. Wu, Z. Gu, Y. Chen, B. Chen, W. Chen, L. Weng, X. Liu, Application of PD-1 blockade in cancer immunotherapy, Comput. Struct. Biotechnol. J. 17 (2019 May 23) 661–674, https://doi.org/10.1016/j.csbj.2019.03.006.